

PROCEEDINGS OF SPIE

SPIEDigitalLibrary.org/conference-proceedings-of-spie

Random walk and graph cut based active contour model for three-dimension interactive pituitary adenoma segmentation from MR images

Min Sun, Xinjian Chen, Zhiqiang Zhang, Chiyuan Ma

Min Sun, Xinjian Chen, Zhiqiang Zhang, Chiyuan Ma, "Random walk and graph cut based active contour model for three-dimension interactive pituitary adenoma segmentation from MR images," Proc. SPIE 10133, Medical Imaging 2017: Image Processing, 101331X (24 February 2017); doi: 10.1117/12.2253990

SPIE.

Event: SPIE Medical Imaging, 2017, Orlando, Florida, United States

Random walk and graph cut based active contour model for three-dimension interactive pituitary adenoma segmentation from MR images

Min Sun^a, Xinjian Chen^{*a}, Zhiqiang Zhang^b, Chiyuan Ma^c

^aSchool of Electronics and Information Engineering, Soochow University, Suzhou, Jiangsu, China 215006; ^bDept. of Medical Imaging, Jinling Hospital, School of Medicine, Nanjing University, Nanjing, Jiangsu, China 210002; ^cDept. of Neurosurgery, Jinling Hospital, School of Medicine, Nanjing University, Nanjing, Jiangsu, China 210002

ABSTRACT

Accurate volume measurements of pituitary adenoma are important to the diagnosis and treatment for this kind of sellar tumor. The pituitary adenomas have different pathological representations and various shapes. Particularly, in the case of infiltrating to surrounding soft tissues, they present similar intensities and indistinct boundary in T1-weighted (T1W) magnetic resonance (MR) images. Then the extraction of pituitary adenoma from MR images is still a challenging task. In this paper, we propose an interactive method to segment the pituitary adenoma from brain MR data, by combining graph cuts based active contour model (GCACM) and random walk algorithm. By using the GCACM method, the segmentation task is formulated as an energy minimization problem by a hybrid active contour model (ACM), and then the problem is solved by the graph cuts method. The region-based term in the hybrid ACM considers the local image intensities as described by Gaussian distributions with different means and variances, expressed as maximum a posteriori probability (MAP). Random walk is utilized as an initialization tool to provide initialized surface for GCACM. The proposed method is evaluated on the three-dimensional (3-D) T1W MR data of 23 patients and compared with the standard graph cuts method, the random walk method, the hybrid ACM method, a GCACM method which considers global mean intensity in region forces, and a competitive region-growing based GrowCut method planted in 3D Slicer. Based on the experimental results, the proposed method is superior to those methods.

Keywords: Image segmentation, graph cut based active contour model (GCACM), random walk, pituitary adenoma, magnetic resonance (MR) images

1. INTRODUCTION

Pituitary adenomas are the most common sellar lesions among all brain tumors¹. In general, clinical classification of pituitary adenoma depends on two terms: size and hormone secretion². Thus the common types of this tumor are microadenoma and macroadenoma according to size, as well as hormone-active and hormone-inactive according to hormone-secretion². Pituitary adenoma volumetry is an important procedure in the diagnosis and clinical efficacy evaluation³⁻⁵. In addition, the volume of pituitary adenoma has been determined to be a dominant relevant factor to the postoperation prognostic assessment of the visual dysfunction, which is a common syndrome due to pituitary adenoma⁶⁻⁹.

In clinic, magnetic resonance (MR) images are used to reveal the size of pituitary adenoma and relative position between the optic chiasm and the tumor because of their high spatial and excellent contrast resolutions¹⁰. For the volume evaluation of pituitary adenoma, the tumor is usually extracted from MR data first, and then the volume result is calculated according to the MR scanning resolution. Three methods are adopted in the recent published papers: manually tracing the tumor's border slice-by-slice on 2-dimensional (2-D) MR scanning of different orientations⁸, semiautomatic segmentation with users' interaction, and complete automatic segmentation. Manual depicting has a high accuracy based on the clinical knowledge of operator. However, it is known to be tiresome, inefficient and subjective. Manual depicting is usually used as ground truth or "gold standard" for the evaluation of computer segmentation algorithm. Automatic segmentation has little manual intervention with great objectivity but often accompanied by training steps, e.g., a label-fusion based method¹¹, which is tedious for needing to develop a vast manual prepared template library. Interactive

semiautomatic segmentation is considered as more appropriate than other two modes for the ability to incorporate user-guided anatomical knowledge and correction into rigid segmentation algorithm¹², e.g., an interactive watershed transform (IWT) after resampling and gradient computation¹³, a competitive region-growing based GrowCut segmentation which has been planted in some software such as 3D Slicer¹⁴, a graph-based method and a balloon inflation method¹⁵⁻¹⁷.

Due to the different pathogenesis and disease progression, pituitary adenomas present various shapes and intensities in T1-weighted (T1W) MR images. In particular, pituitary adenomas grow upward compressing the optic chiasm or infiltrating to surrounding soft tissues, which demonstrate similar intensities and indistinct boundaries, making the segmentation of pituitary adenoma still be a hard task. In recent years, graph cuts based active contour models (GCACM) are presented with the inspiration from the geocuts algorithm proposed by Boykov et al.¹⁸ Graph cuts acquire global optimal solutions for minimal energy in the graphs which is constructed according to the image information, and separate the objects from background through setting different labels to nodes according to sinks and sources respectively^{19,20}. The metrication artifacts in boundaries obtained by graph cuts are inherent due to the discrete graph formulation, which are influenced by the size of the neighborhood system used in the graph construction, choosing larger neighborhood system generally produces smoother segmentation results^{18, 21}. Active contour models (ACM) have the drawbacks such as easily trapping to local minima and being sensitive to the position of initial contour as well as noise, but they can produce continuous contours separating the image into different parts with minimal geometric artifacts^{22,23}. GCACM combines the advantages of these two standard segmentation methods. In this method, ACM are usually reformulated in discrete frameworks and are solved by graph cuts. The length of the evolving contour (geodesic active contour) in the energy function is presented by the equivalent cut metric for the Riemannian length, as shown in the works of El-Zehiry et al.^{24,25}, Tao et al.²⁶, Bae et al.²⁷, Zheng et al.^{28,29}, etc.

In this paper, we propose an interactive method to segment the pituitary adenoma from three-dimensional (3-D) T1-weighted (T1W) MR data, by combining GCACM and random walk (RW) algorithm. By using GCACM method, the segmentation task is formulated as an energy minimization problem by a hybrid ACM, and then the problem is solved by max-flow/min-cut method. The region-based term in the hybrid ACM considers the local image intensities as described by Gaussian distributions with different means and variances. Random walk is used to provide initialized surface for GCACM with user-guided seeds.

The paper is organized as follows. Section 2 shows the flowchart of the proposed method and discusses the formulation and discretization of the hybrid ACM. Section 3 presents the construction of the graph and the experimental details of the proposed approach. Section 4 discusses the experimental results and concludes the paper. Section 5 expresses thanks to the projects and funding supporting this study.

2. DISCRETIZATION FOR THE ACM FORMULATION

The proposed method includes three major parts: obtaining initialized closed surface for GCACM by using the RW algorithm with user defined seeds, performing iterative segmentation with GCACM method and post-processing with 3-D median filter (shown in Figure 1). In the proposed framework, a new hybrid ACM is designed to formulate the segmentation task as an energy minimization problem. Then the hybrid ACM is discretized according to the graph construction and solved by max-flow/min-cut method. Iterative segmentation is performed until the results converge. Finally, the evolution surface is smoothed by a 3-D median filter.

2.1 Hybrid ACM formulation

The hybrid ACM combining edge information and region information of image usually has energy formulation as follows:

$$E = E_{Edge} + E_{Region} \quad (1)$$

In this paper, we consider the geodesic active contours (GAC) as edge-based energy term E_{Edge} using the classical formulation of GAC model. The region-based energy term considers the local image intensities as described by Gaussian distributions with different means and variances, expressed as maximum a posteriori probability (MAP) form. Given the image domain $\Omega \subset R^2$, let $I(x) : \Omega \rightarrow R$ be a specific image. Length of the closed curve C which divides the image into two independent parts is denoted as $L(C)$. Let the set inside C be Ω_1 and the set outside C be Ω_2 . For each point x in the image domain Ω , we consider a circular neighborhood with a small radius ρ , which is defined as $O_x = \{y : |x - y| \leq \rho\}$, as shown in Figure 2.

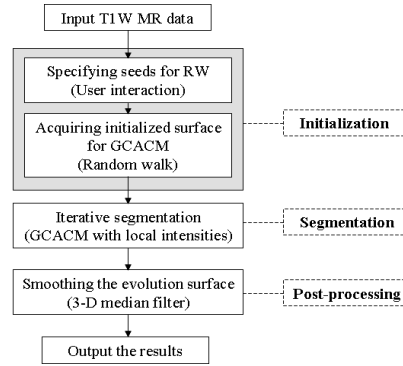


Figure 1. Flowchart of the proposed method.

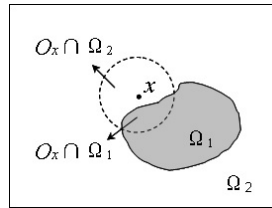


Figure 2. Graphical representation of $O_x \cap \Omega_i$. The dashed circle represents the neighborhood of x .

The probability density of a given pixel in region $O_x \cap \Omega_i$ is denoted as $p_{\Omega_i}(x, y)$:

$$p_{\Omega_i}(x, y) = \frac{1}{\sqrt{2\pi}\sigma_i(x)} \exp\left(-\frac{(u_i(x) - I(y))^2}{2\sigma_i(x)^2}\right), i = 1, 2 \quad (2)$$

where $u_i(x)$ and $\sigma_i(x)$ are the local intensity means and standard deviations in the region $O_x \cap \Omega_i$ of each point x , respectively. The energy function that combines the edge-based energy and the region-based energy can be written as:

$$E = E_{Edge} + E_{Region} = \int_0^{L(c)} g(\nabla I(c(s))) ds + \sum_{i=1}^2 \iint_{\Omega_i} [-w(x, y) \log p_{\Omega_i}(x, y)] dy dx \quad (3)$$

$$= \int_0^{L(c)} \frac{1}{1 + \beta |\nabla I(c(s))|} ds - \iint_{\Omega_1} w(x, y) \log p_{\Omega_1}(x, y) dx dy - \iint_{\Omega_2} w(x, y) \log p_{\Omega_2}(x, y) dx dy$$

where β is an arbitrary positive constant. Function w is a weighting function that assigns larger weights to the data $I(y)$ for y closer to the center x of the neighborhood O_x . In this paper, the weighting function w is a truncated Gaussian kernel as described by Eq. 4:

$$w(x, y) = \begin{cases} \frac{1}{\alpha} \exp\left(-\frac{|x-y|^2}{2\sigma^2}\right), & \text{if } |x-y| \leq \rho \\ 0, & \text{if } |x-y| > \rho \end{cases} \quad (4)$$

where α is a constant such that $\int w(x, y) = 1$.

2.2 Discrete formulation for the hybrid ACM

To provide a discrete formulation for the hybrid ACM, we define a binary variable x_p associating with a voxel p to replace the Heaviside step function of the distance map in continuous optimization frameworks, such as:

$$x_p = \begin{cases} 1, & p \in Object \\ 0, & p \in Background \end{cases} \quad (5)$$

We assign a value of 1 to x_p if p is connected to the sink T and 0 if it is connected to the source S .

With the cut metric for the Euclidean curve length presented in Ref. [18], the discrete formulation of edge-based energy E_{Edge} can be given using the same discrete graph cut formulation in Ref. [26], as follows:

$$E_{Edge}(p, q) = \sum_p \sum_{q \in N(p)} \frac{\omega_{pq}((1-x_p)x_q + x_p(1-x_q))}{1 + \beta|I(p) - I(q)|} \quad (6)$$

where ω_{pq} is the nonnegative weights on the edges¹⁸. We use its 3-D form and set it equal to $\pi/4$ in this study.

The discrete form of region-based energy E_{Region} can be described as follows:

$$\begin{aligned} E_{Region}(p) &= E_s(p) + E_t(p) \\ &= \sum_p \sum_{q \in N(p)} w(p-q) \left(\log \sigma_s(p) + \frac{(u_s(p) - I(q))^2}{2\sigma_s(p)^2} \right) (1-x_q) + \sum_p \sum_{q \in N(p)} w(p-q) \left(\log \sigma_t(p) + \frac{(u_t(p) - I(q))^2}{2\sigma_t(p)^2} \right) x_q \end{aligned} \quad (7)$$

where $u_s(p)$, $u_t(p)$ and $\sigma_s(p)$, $\sigma_t(p)$ are the discrete forms of $u_i(x)$ and $\sigma_i(x)$ with such formulas as followings:

$$\begin{cases} u_s(p) = \frac{\sum_q w(p-q) I(q) (1-x_q)}{\sum_q w(p-q) (1-x_q)} \\ u_t(p) = \frac{\sum_q w(p-q) I(q) x_q}{\sum_q w(p-q) x_q} \end{cases} \quad (8)$$

$$\begin{cases} \sigma_s(p) = \frac{\sum_q w(p-q) (u_s(p) - I(q))^2 (1-x_q)}{\sum_q w(p-q) (1-x_q)} \\ \sigma_t(p) = \frac{\sum_q w(p-q) (u_t(p) - I(q))^2 x_q}{\sum_q w(p-q) x_q} \end{cases} \quad (9)$$

To avoid the region and edge balance problem in the standard combinatorial form of graph cuts method, we use the multiplicative formulation proposed in Ref. [28] and Ref. [29]. So the energy function of the modified GCACM for pituitary adenoma MR image segmentation can be defined as:

$$E = E_{Edge}(p, q) \cdot E'_{Region}(p) \quad (10)$$

$$E'_{Region}(p) = \sum_p \min(|E_s(p) + E_t(q)|, |E_s(q) + E_t(p)|) \quad (11)$$

If neighbor voxels p , q are either inside or outside the object simultaneously, then $|E_s(p) + E_t(q)| > 0$ and $|E_s(q) + E_t(p)| > 0$. If neighbor voxels p , q are on the different side of the object's boundary, then $|E_s(p) + E_t(q)| \approx 0$ or $|E_s(q) + E_t(p)| \approx 0$. Therefore, the Eq.10 can be minimized only when neighbor voxels p , q are on the boundary of the object.

3. INITIALIZATION AND IMAGE SEGMENTATION

3.1 Initialization with the RW method

Location of initialized surface greatly influences the segmentation results of GCACM method, which is demanded to be placed near and inside the true boundary of the object²⁹. In this paper, we use the RW algorithm to product the initialized surface with a user specified foreground seed inside pituitary adenoma body and a background seed in the dark marginal area. According to the RW method, the probability maps associated with each label denote the probabilities that a random walker starting from each unlabeled voxel will firstly reach one of the prelabeled voxels³⁰. RW obtains the image segmentation by assigning the same label to each voxel with the seed which has the greatest probability. With an appropriate threshold derived by expectation maximization (EM) algorithm, the voxels which most likely to belong to the object are segmented from the probability map, and then they will be used as the foreground seeds for the GCACM method. The boundary of the segmented voxels is set as the initialized surface.

3.2 Graph construction

A special graph for the energy minimization optimization is constructed to segment pituitary adenoma from 3-D MR images. To reduce the computational complexity, we use 6-neighborhood system to identify all the neighboring voxels q for each voxel p in the 3-D MR data. For n -link, the edges connecting neighboring voxels are weighted with $E_{Edge}(p, q) \cdot E'_{Region}(p)$ in the graph. For t -link, If $|E_s(p)| > |E_t(p)|$ and $x_p=1$, add link pT with weight infinite, and if $|E_s(p)| < |E_t(p)|$ and $x_p=0$, add link pS with weight infinite.

3.3 Procedure of the pituitary adenoma segmentation

Procedure of the proposed pituitary adenoma segmentation method can be summarized as follows:

1. Obtaining the initialized surface S_{ur} with the RW method. Initializing the binary variable $x_p=1$ if p is inside S_{ur} , and $x_p=0$ if p is outside S_{ur} .
2. Calculating $u_s(p), u_t(p)$ and $\sigma_s(p), \sigma_t(p)$ using Eq.8 and Eq.9.
3. Constructing the graph for the proposed energy Eq.10 as described above.
4. Calculating the minimum cut on the constructed graph by the maxflow/min-cut algorithm, then updating the binary variable x_p definition according to the calculation results.
5. Smoothing the evolution surface with 3-D median filter.
6. Repeating steps 2–5 until convergence.

4. EXPERIMENT RESULTS AND CONCLUSIONS

We implement the initialization and iterative procedures in MATLAB R2012a (The MathWorks Inc., Natick, USA) and the maxflow/min-cut algorithm in C++. As is known, the computational complexity of the RW method greatly increase and the segmentation speed slow down sharply along with the pixel/voxel number increasement. In addition, the max-flow/min-cut algorithm has the complexity $O(mn^2|C|)$, where the $|C|$ is the cost of the minimum cut, m is the number of nodes, and n is the number of edges. Considering reducing the computational complexity, we firstly cut out a cuboid with size of $71 \times 71 \times 61$ empirically from the 3-D data centered on a point, which is defined inside the pituitary adenoma body on a slice near the center of the tumor in terms of the anatomical prior knowledge. The point is also used as the foreground seed for the RW algorithm, and a user defined point in dark region is used as the background seed. The process of acquiring initialized surface is presented on a sagittal view MR cross-section near the center of pituitary adenoma, as shown in Figure 3 a and b.

In the quantitative evaluation of the proposed method, we use manual delineating boundaries as gold standard in the measurement of Dice similarity coefficient (DSC). Manual segmentations are performed by neurological surgeons with several years of experiences in the resection of brain tumors using ITK-SNAP 3.2.0 (<http://www.itksnap.org>). The DSC is defined as the relative volume overlap between experiment results V_E and gold standard V_G .

$$DSC = 1 - \frac{|V_G - V_E|}{V_G} \quad (12)$$

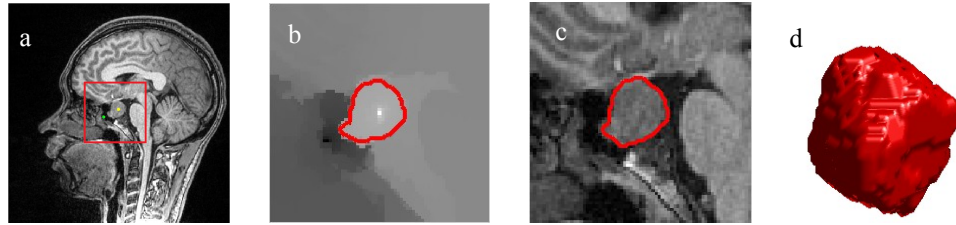


Figure 3. Demonstration of the surface initialization for the proposed method. a. A user specified foreground seed (yellow dot) and a background seed (green dot) are superimposed on the original image. Red rectangular frame denotes the range of cut-off. b. Initialized contour superimposed on the probabilities map. Note that brighter intensity indicates higher probability. c. Segmented contour superimposed on the cropped original image. d. 3-D rendering of the resulting segmentation.

4.1 Experiment results

The segmentation results obtained by the proposed method are shown in Figure 3 c and d. Figure 4 shows the segmentation results obtained by the proposed method, the RW algorithm, the graph cuts method, a hybrid ACM method presented in Ref. [31], a similar GCACM method which uses mean intensity of each partition in region-based energy of ACM as described in Ref. [28], and a competitive region-growing based GrowCut segmentation which has been planted in some software such as 3D Slicer (<http://www.slicer.org>) described in Ref. [14]. To evaluate the significance and effectiveness of the combination of these methods, we conduct these methods on same data sets respectively and compare their results with the DSC values. In the comparison, the same foreground and background seeds for the RW method and proposed method are shown in Figure 4 a. Same initial surfaces for the hybrid ACM and GCACM are used as initialization, which are regular spheres generated from a point centered at the tumor on the sagittal view MR slice near the center of pituitary adenoma with user defined radii, as shown in Figure 4 e. In order to fully show the effectiveness of graph cuts method and the GrowCut method, we operate them on the same pituitary adenoma MR data with more precise seeds setting.

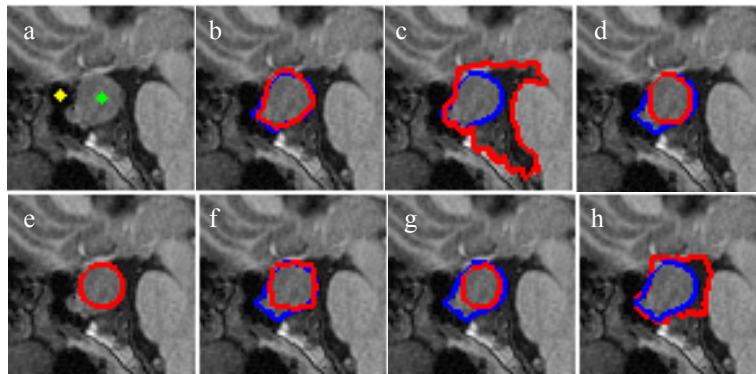


Figure 4. Segmentation results of six segmentation methods applied on a set of 3-D T1W MR images of pituitary adenoma with irregular shape and non-compression to optic chiasm. a. User defined seeds are superimposed on the cut-off image from a sagittal view cross-section near the center of pituitary adenoma. Green dot and yellow dot denote foreground and background seeds respectively. b. Results obtained by the proposed method with the seeds defined in a. c. Results obtained by the RW method with the seeds defined in a. d. Results obtained by the graph cuts method with more seeds than those defined in a. e. A profile of initial spherical surface for the hybrid ACM and GCACM method is superimposed on the cropped image. f. Results obtained by a hybrid ACM method described in Ref. [31]. g. Results obtained by a GCACM method described in Ref. [28]. h. Results obtained by GrowCut method planted in 3D Slicer as described in Ref. [14] with precise seeds setting. Red contours represent the segmentation results and blue contours represent the ground truth in (b)-(d) and (f)-(h).

Table 1 gives the summary of experiment results for 23 pituitary adenomas in the means of minimum value, maximum value, mean and standard deviation of DSC. Comparisons between the proposed method and five typical segmentation frameworks are also presented in the Table 1. The experiments demonstrate that the proposed method performs best among these methods, achieving highest mean values of DSC (88.36%). The RW method (with the mean values 79.44% of DSC) takes the second place, which is followed in descending order by GCACM in Ref. [28], hybrid

ACM in Ref. [31], and graph cuts in all cases. Additionally, the GrowCut in Ref. [14] performs also well with more precise interactive seeds setting.

Table 1. DSC results of the proposed method and five published segmentation frameworks.

Results	Proposed method	RW	Graph cuts	ACM in [31]	GCACM in [28]	GrowCut in [14]
min	74.86%	65.71%	0.69%	47.67%	49.45%	67.62%
max	93.35%	89.24%	83.35%	85.88%	78.55%	89.07%
mean \pm SD	88.36% \pm 5.61%	79.44% \pm 5.23%	21.91% \pm 24.41%	70.87% \pm 9.36%	70.88% \pm 8.08%	81.61% \pm 7.37%

4.2 Conclusions

The proposed method is a comprehensive 3-D method to interactively segment pituitary adenoma by combining the RW method, the graph cuts, and the hybrid ACM, making fully use of their advantages. All of these three standard segmentation methods are energy-based and semi-supervised, needing users to provide the information of objects to minimize the energy function and acquire the image partition. Experiments shown above demonstrate their abilities to extract the interest regions respectively. More seeds and precise initializations may distinctly improve their segmentation accuracy, however, the increased vast user interaction and huge computation will become great burdens.

The proposed method uses the RW method to obtain an appropriate initialized closed surface with only two user defined seeds, greatly reducing the labor burden. In the hybrid ACM formulation, the propose method adopts Gaussian distributions to describe the local image intensity for the region-based energy, thus it can deal with the intensity inhomogeneous inside pituitary adenoma body, avoiding error segmentation of the tissues with similar intensities around the tumour. The visual and quantitative results show that the proposed method is superior to other typical published segmentation methods. It can provide clinicians with accurate volumetric information of pituitary adenoma to assist diagnose and treatment.

5. ACKNOWLEDGMENTS

This work is supported in part by the National Basic Research Program of China (973 Program) under Grant 2014CB748600, and in part by the National Natural Science Foundation of China (NSFC) under Grant 81371629, 81401472, 61401294, 6140293, 61622114, and in part by Natural Science Foundation of the Jiangsu Province under Grant BK20140052.

REFERENCES

- [1] McNicol, A. M., "Pituitary adenomas," *Histopathology* 11 (10), 995-1011 (1987).
- [2] Al-Shraim, M. and Asa, S. L., "The 2004 World Health Organization classification of pituitary tumors: What is new? " *Acta Neuropathol.* 111 (1), 1-7 (2006).
- [3] McIlwaine, G. G., Carrim, Z. I., Lueck, C. J. and Chrisp, T. M., "A mechanical theory to account for bitemporal hemianopia from chiasmal compression," *J. Neuroophthalmol.* 25 (1), 40-43 (2005).
- [4] Mayson, S. E. and Snyder, P. J., "Silent (clinically nonfunctioning) pituitary adenomas," *J. Neurooncol.* 117 (3), 429-436 (2014).
- [5] Sharma, B. S., Sinha, S. and Suri, A., "Treatment of giant pituitary adenomas," *Neurosurg. Q.* 17 (2), 120-127 (2007).
- [6] Okamoto, Y., Okamoto, F., Yamada, S., Honda, M., Hiraoka, T. and Oshika, T., "Vision-related quality of life after transsphenoidal surgery for pituitary adenoma," *Invest. Ophthalmol. Visual Sci.* 51 (7), 3405-3410 (2010).
- [7] Barzaghi, L. R., Medone, M., Losa, M., Bianchi, S., Giovanelli, M. and Mortini, P., "Prognostic factors of visual field improvement after trans-sphenoidal approach for pituitary macroadenomas: review of the literature and analysis by quantitative method," *Neurosurg. Rev.* 35 (3), 369-378 (2012).
- [8] Monteiro, M. L. R., Zambon, B. K. and Cunha, L. P., "Predictive factors for the development of visual loss in patients with pituitary macroadenomas and for visual recovery after optic pathway decompression," *Can. J. Ophthalmol.* 45 (4), 404-408 (2010).

- [9] Ho, R. W., Huang, H. M. and Ho, J. T., "The influence of pituitary adenoma size on vision and visual outcomes after trans-sphenoidal adenectomy : A report of 78 cases," *J. Korean Neurosurg. Soc.* 57 (1), 23-31 (2015).
- [10] Miki, Y., Matsuo, M., Nishizawa, S., Kuroda, Y., Keyaki, A., Makita, Y. and Kawamura, J., "Pituitary adenomas and normal pituitary tissue: enhancement patterns on gadopentetate-enhanced MR imaging," *Radiology* 177 (1), 35–38 (1990).
- [11] Wong, A. P. Y., Pipitone, J., Park, M. T. M., et al., "Estimating volumes of the pituitary gland from T1-weighted magnetic-resonance images: Effects of age, puberty, testosterone, and estradiol," *Neuroimage* 94, 216-221 (2014).
- [12] McGuinness, K. and O'Connor, N. E., "A comparative evaluation of interactive segmentation algorithms," *Pattern Recognit.* 43(2), 434–444 (2010).
- [13] Renz, D. M., Hahn, H. K., Schmidt, P., et al., "Accuracy and reproducibility of a novel semi-automatic segmentation technique for MR volumetry of the pituitary gland," *Neuroradiology* 53 (4), 233–244 (2011).
- [14] Egger, J., Kapur, T., Nimsy, C. and Kikinis, R., "Pituitary adenoma volumetry with 3D slicer," *PLoS One* 7(12), e51788 (2012).
- [15] Egger, J., Zukic, D., Freisleben, B., Kolb, A. and Nimsy, C., "Segmentation of pituitary adenoma: A graph-based method vs. a balloon inflation method," *Comput. Methods Programs Biomed.* 110 (3), 268–278 (2013).
- [16] Egger, J., Bauer, M. H. A., Kuhnt, D., Freisleben, B. and Nimsy, C., "Pituitary adenoma segmentation," *Proc. Biosignal*, 2010.
- [17] Davies, B. M., Carr, E., Soh, C. and Gnanalingham, K. K., "Assessing size of pituitary adenomas: a comparison of qualitative and quantitative methods on MR," *Acta Neurochir.* 158 (4), 677-683 (2016).
- [18] Boykov, Y. and Kolmogorov, V., "Computing geodesics and minimal surfaces via graph cuts," *Proc. ICCV*, 26-33 (2003).
- [19] Boykov, Y., Veksler, O. and Zabih, R., "Fast approximate energy minimization via graph cuts," *IEEE Trans. Pattern Anal. Mach. Intell.* 23 (11), 1222-1239 (2001).
- [20] Boykov, Y. and Kolmogorov, V., "An experimental comparison of min-cut/max-flow algorithms for energy minimization in vision," *IEEE Trans. Pattern Anal. Mach. Intell.* 26(9), 1124-1137 (2004).
- [21] Xu, N., Ahuja, N. and Bansal, R., "Object segmentation using graph cuts based active contours," *Comput. Vis. Image Underst.* 107 (3), 210–224 (2007).
- [22] Caselles, V., Kimmel, R. and Sapiro, G., "Geodesic active contours," *Int. J. Comput. Vis.* 1 (22), 61-79 (1997).
- [23] Cui, H. and Gao, L., "Geodesic active contour, inertia and initial speed," *Pattern Recognit. Lett.* 2008.
- [24] El-Zehiry, N. and Elmaghraby, A., "A graph cut based active contour without edges with relaxed homogeneity constraint," *Proc. ICPR*, 1-4 (2008).
- [25] El-Zehiry, N. and Elmaghraby, A., "A graph cut based active contour for multiphase image segmentation," *Proc. ICIP*, 3188-3191 (2008).
- [26] Tao, W., "Iterative narrowband-based graph cuts optimization for geodesic active contours with region forces (GACWRF)," *IEEE Trans. Image Process.* 21(1), 284-296 (2012).
- [27] Bae, E. and Tai, X., "Graph cut optimization for the piecewise constant level set method applied to multiphase image segmentation," *Proc. SSVM LNCS* 5567, 1-13 (2009).
- [28] Zheng, Q., Dong, E. and Cao, Z., "Graph cuts based active contour model with selective local or global segmentation," *Electron. Lett.* 48 (9), 490-491 (2012).
- [29] Zheng, Q., Dong, E. and Cao, Z., "Modified localized graph cuts based active contour model for local segmentation with surrounding nearby clutter and intensity inhomogeneity," *Signal Process.* 93 (4), 961-966 (2013).
- [30] Grady, L., "Random walks for image segmentation," *IEEE Trans. Patten Anal. Mach. Intell.* 28 (11), 1768-1783 (2006).
- [31] Zhang, Y., Matuszewski, B. J., Shark, L. and Moore, C. J., "Medical image segmentation using new hybrid level-set method," *Proc. MEDIVIS*, 71-76 (2008).